Virology 378 (2008) 133–141

Contents lists available at ScienceDirect

Virology

journal homepage: www.elsevier.com/locate/yviro

Mutations that alter a repeated ACCA element located at the 5′ end of the *Potato virus X* genome affect RNA accumulation ☆

Mi-Ri Park [a], Sun-Jung Kwon [b], Hong-Soo Choi [c], Cynthia L. Hemenway [d,*], Kook-Hyung Kim [a,b,*]

[a] *Department of Agricultural Biotechnology and Center for Plant Molecular Genetics and Breeding Research, Seoul National University, Seoul 151-921, Korea*
[b] *Research Institute for Agriculture and Life Sciences, Seoul National University, Seoul 151-921, Korea*
[c] *Department of Plant Pathology, National Institute of Agricultural Science and Technology, Suwon 441-707, Korea*
[d] *Department of Molecular and Structural Biochemistry, Box 7622, North Carolina State University, Raleigh, North Carolina 27695-7622, USA*

ARTICLE INFO

Article history:
Received 25 March 2008
Returned to author for revision
8 April 2008
Accepted 8 May 2008
Available online 26 June 2008

Keywords:
PVX
ACCA elements
RNA interaction
Replication

ABSTRACT

The repeated ACCA or AC-rich sequence and structural (SL1) elements in the 5′ non-translated region (NTR) of the *Potato virus X* (PVX) RNA play vital roles in the PVX life cycle by controlling translation, RNA replication, movement, and assembly. It has already been shown that the repeated ACCA or AC-rich sequence affect both gRNA and sgRNA accumulation, while not affecting minus-strand RNA accumulation, and are also required for host protein binding. The functional significance of the repeated ACCA sequence elements in the 5′ NTR region was investigated by analyzing the effects of deletion and site-directed mutations on PVX replication in *Nicotiana benthamiana* plants and NT1 protoplasts. Substitution (ACCA into AAAA or UUUU) mutations introduced in the first (nt 10–13) element in the 5′ NTR of the PVX RNA significantly affected viral replication, while mutations introduced in the second (nt 17–20) and third (nt 20–23) elements did not. The fourth (nt 29–32) ACCA element weakly affected virus replication, whereas mutations in the fifth (nt 38–41) significantly reduced virus replication due to the structure disruption of SL1 by AAAA and/or UUUU substitutions. Further characterization of the first ACCA element indicated that duplication of ACCA at nt 10–13 (nt 10–17, ACCAACCA) caused severe symptom development as compared to that of wild type, while deletion of the single element (nt 10–13), ΔACCA) or tripling of this element caused reduced symptom development. Single- and double-nucleotide substitutions introduced into the first ACCA element revealed the importance of CC located at nt positions 11 and 12. Altogether, these results indicate that the first ACCA element is important for PVX replication.

Introduction

Potato virus X (PVX), the type member of the *Potexvirus* genus, is a flexuous rod-shaped virus containing a 6.4 kb plus-stranded RNA genome (Bercks, 1970; Huisman et al., 1988). The PVX genome, which is capped and polyadenylated, consists of an 84 nucleotide (nt) 5′ non-translated region (NTR), five open reading frames (ORFs), and a 72 nt 3′ NTR (Bercks, 1970; Huisman et al., 1988; Skryabin et al., 1988; Fig. 1). ORF1 encodes the viral replicase protein (165 kDa), which is the only viral protein absolutely required for PVX RNA synthesis. This replicase exhibits the methyltransferase/helicase/polymerase arrangement found in all nonsegmented viruses of the Sindbis-like supergroup (Rozanov et al., 1992). The function of viral cell-to-cell transport is associated with the triple gene block (TGB), ORFs 2–4 (Argos et al., 1980; Bercks, 1970), and the product of ORF5, coat protein (CP), is involved in both virus movement and encapsidation (Chapman et al., 1992; Oparka et al., 1996). During PVX infection, proteins derived from these ORFs as well as genomic-length plus- and minus-strand RNAs, several sgRNAs, and corresponding double-stranded RNAs are produced (Dolja et al., 1987; Price, 1992). The two major sgRNAs are uitlized for expression of the first TGB gene (ORF2) and CP, respectively, whereas the other two TGB genes (ORFs 3 and 4) are expressed from a less-abundant sgRNA (Morozov et al., 1991; Verchot et al., 1998).

The 5′ PVX NTR contains multiple *cis*-acting regulatory signals, including AC-rich sequences and several repeat ACCA motifs (Kim and Hemenway, 1996) followed by at least one stable stem-loop, SL1 (Miller et al., 1998), all of which are important for both gRNA and sgRNA accumulation in NT1 protoplasts. Further progeny viral RNA analysis of the SL1 mutants through several passages also indicated the selection of the original SL1 structure (Miller et al., 1999). Kwon et al. (2005) demonstrated that the CP-binding element is also located within this SL1 structure at the 5′ region and that the binding of CP subunits to the SL1 structure was sufficient for the formation of virus like particles. Recently, it was further confirmed that the 5′-terminal region of PVX RNA was encapsidated selectively in single-tailed RNA-CP particles and

☆ The English in this document has been checked by at least two professional editors, both native speakers of English. For a certificate, see: http://www.textcheck.com/cgi-bin/certificate.cgi?id=ZWNDjq.

* Corresponding authors. K.-H. Kim is to be contacted at Department of Agricultural Biotechnology and Center for Plant Molecular Genetics and Breeding Research, Seoul National University, Seoul 151-921, Korea. Fax: +82 2 873 2317.
E-mail address: kookkim@snu.ac.kr (K.-H. Kim).

0042-6822/$ – see front matter © 2008 Elsevier Inc. All rights reserved.
doi:10.1016/j.virol.2008.05.004

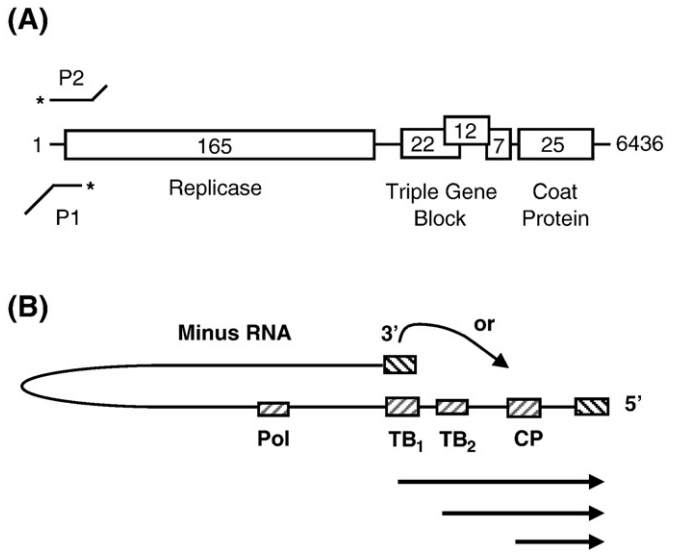

Fig. 1. Schematic representation of the PVX genome (A) and model for long-distance interactions required for PVX replication (B). The five ORFs are denoted by open boxes and are labeled according to the sizes of the predicted polypeptides. The relative positions of the plus-strand RNA probe (P1) and minus-strand RNA probe (P2) for S1 nuclease protection assays are indicated; asterisks denote ^{32}P-labeled positions. The shown is one possible long-distance interaction. Positions and sequences of *cis*-acting elements defined here and previously (Hu et al., 2007; Kim and Hemenway, 1997, 1999). The products of plus-strand sgRNA synthesis, including TB sgRNA (TB1), CP sgRNA (CP), and the putative sgRNA initiating near ORF3 (TB2) are also shown.

modulate the nature of the infectious virus transport form through the binding with TGBp1 (Karpova et al., 2006). In view of the involvement of the 5′-terminal region of PVX RNA in movement or transport, it was shown that a SL1 structure was also acts as a *cis*-acting element essential for cell-to-cell movement of RNA and suggests the coordinated nature of RNA replication and RNA movement (Lough et al., 2006).

Although the 5′ 31 nt containing repeated ACCA motifs are predicted to be unstructured, sequence elements in this region have also been to be important for PVX accumulation (Kim and Hemenway, 1996, 1999; Miller et al., 1999). A cellular protein of about 54 kDa (p54) binds to sequences in the 5′ proximal 46 nt of the PVX RNA genome that may be involved in the accumulation of PVX plus-strand RNA (Kim et al., 2002). Site-directed mutations introduced within this 46 nt region further indicated that an ACCA sequence element located at nt 10–13 was important for optimal binding, suggesting the functional importance of p54 binding to the 5′ terminus of the viral genomic RNA in PVX RNA replication. In addition, mutations that decreased the affinity of the template RNA for the cellular factor decreased PVX plus-strand RNA accumulation in protoplasts (Kim et al., 2002). Kim and Hemenway (1997) showed that conserved octanucleotide sequence elements located upstream of the two major PVX sgRNAs are important for sgRNA accumulation in protoplasts and potentially some other aspect of the infection process in plants. Complementarity between the 5′ terminus (or 3′ terminus of minus-strand RNA) and the conserved octanucleotide elements is important for both genomic and subgenomic plus-strand RNA accumulation (Kim and Hemenway, 1997). Recently, Hu et al. (2007) have shown that these conserved octanucleotide elements are also required for optimal transcription of minus-strand RNA both *in vitro* and *in vivo*. Altogether, these data suggest the dynamic interactions of various RNA elements at both termini and the internal octanucleotide during PVX replication (Fig. 1).

Since the binding of the cellular protein to the 5′ end of the plus-strand RNA and virus replication on inoculated protoplasts were closely co-related, it is tempting to speculate that essentiality of sequences on 5′ end of plus-strand RNA is in part due to the binding of

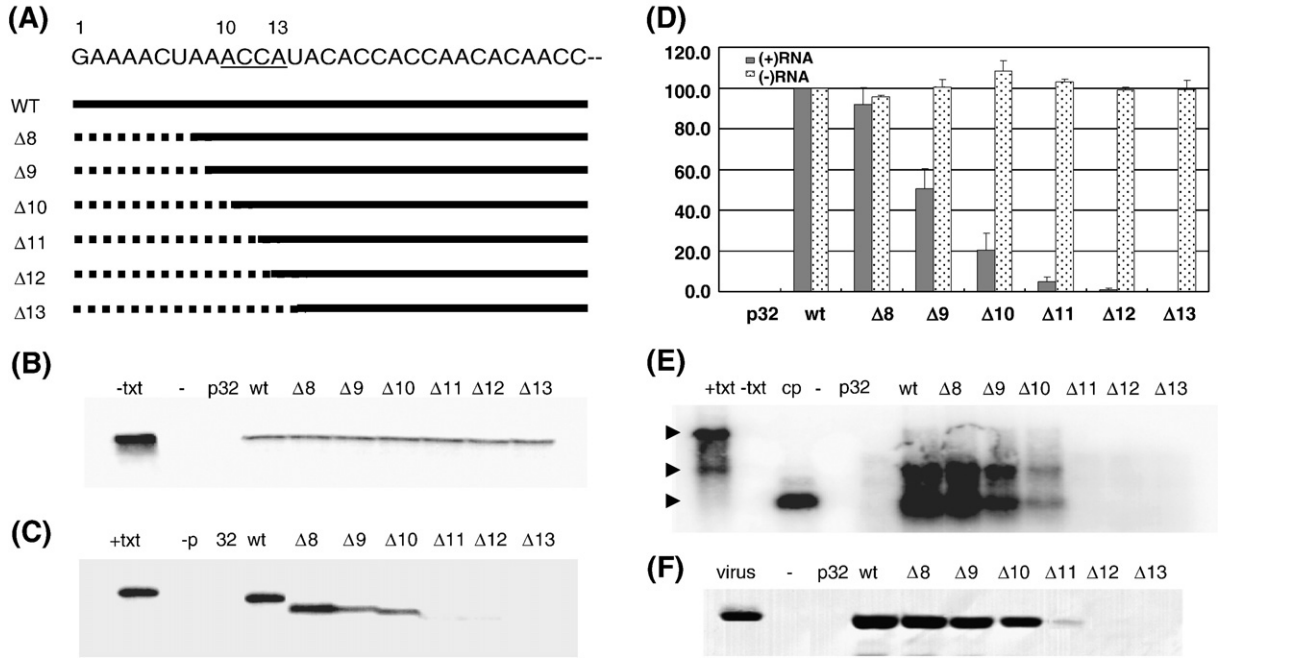

Fig. 2. Effects of mutations introduced into PVX genomic RNA on viral replication in *N. tabacum* NT1 protoplasts. (A) Schematic representation of deletion mutations made in nt 1–13 of the genomic RNA. Deletions from the 5′ end are indicated by dotted lines. (B and C) Effect of mutation on PVX plus- and minus-strand RNA accumulation using S1 nuclease protection assays. Accumulation of minus-strand (B) and plus-strand (C) RNA inoculated with negative control transcripts p32, positive control pMON8453 (wt), and transcripts containing mutations in the 5′ NTR (Δ8, Δ9, Δ10, Δ11, Δ12, and Δ13) in protoplasts. The first lane in C and D contains protected fragments obtained by hybridization to minus-strand (−txt) and plus-strand (+txt) RNA transcripts, respectively. (D) Accumulation of plus- and (closed bar) minus-strand (shaded bar) RNA on PVX mutants. RNA levels were measured using a Molecular Dynamics Photoimager. Each value is the mean compared to that of the wild type as a percentage of the wild type and the standard error compiled from at least six and three independent experiments for plus- and minus-strand RNA accumulation, respectively. (E) Accumulation of subgenomic RNA and (F) CP subunits, respectively, inoculated with negative control transcript p32 and positive control pMON8453 (wt), and transcripts containing mutations in the 5′ NTR (Δ8, Δ9, Δ10, Δ11, Δ12, and Δ13) in protoplasts. The first, second, and third lanes in F contain detected bands obtained by Northern blotting with the PVX CP probe to plus-strand (+txt) and minus-strand (−txt) RNA and CP transcripts. The first lane in G contains the detected band obtained using Western blotting with antiserum prepared against purified PVX.

Table 1
Accumulation of plus- and minus-strand RNA on PVX mutants in *N. tabacum* NT1 protoplasts

Mutants	(+) RNA[a]	(−) RNA[a]
wt	100.0 a	100.0 ab
p32	0.0 d	0.0 c
Δ8	92.0 a	96.0 b
Δ9	50.5 b	100.4 ab
Δ10	20.4 c	108.6 a
Δ11	5.0 cd	102.9 ab
Δ12	0.8 d	98.8 ab
Δ13	0.0 d	99.3 ab

[a] Data were analyzed by ANOVA and means were compared using the Fisher's LSD test using SAS program (version 9.1). Means with the same letter are not significantly different at $P \leq 0.05$.

the cellular protein. In this study, to further assess the importance of the repeated ACCA motifs in the 5′ PVX NTR for viral replication, we have analyzed the functional significance of these repeated ACCA-motifs by introducing deletions and site-directed mutations within the repeated ACCA sequences and by inoculating transcripts containing mutations onto NT1 protoplasts and *Nicotiana benthamiana* plants.

Results

Effects of mutations in the first ACCA (nt 10–13) element on PVX replication

We have previously reported that deletion of the nucleotide sequence between nt 8 and 13, containing the first ACCA element, affects PVX plus-strand RNA synthesis in NT1 protoplasts (Kim and Hemenway, 1996). The result showed that plus-strand genomic RNA accumulation was reduced by these mutants as contrast with minus-strand genomic RNA accumulation. We have also previously reported that changing the first ACCA to AAAA, AUUA, or UUUU significantly reduced PVX plus-strand RNA accumulation in inoculated NT1 protoplasts, while no deleterious effect was evident when protoplasts were inoculated with a GGGG version of this element (Kim et al., 2002).

To further define the role of the first ACCA (10–13) element in genomic RNA synthesis, we analyzed several incremental deletions in the 5′ NTR (Δ8, Δ9, Δ10, Δ11, Δ12 and Δ13) (Fig. 2A). The effects of each mutation on PVX replication were assayed by inoculating wild-type and mutant transcripts onto NT1 protoplasts and subsequently analyzed by S1 nuclease protection assays for quantification of with plus- and minus-strand RNA using probes P1 and P2, respectively (Fig. 1A) and by western and northern blot analyses.

As shown in Figs. 2C and D, accumulation of plus-strand RNA levels were significantly decreased with increasing deletions from the 5′ end, and was almost undetectable with deletion of 11 (5% compared to that of wt) or more nt (0.8% and 0% for Δ12 and Δ13, respectively, compared to that of wt, Table 1). As expected, minus-strand RNA accumulation was not affected by any of the deletion mutants (Fig. 2B and Table 1). The accumulation of sgRNAs, as measured by northern analyses, also decreased with increasing deletion from the 5′ terminus, and was not detectable with deletion of 11 or more nt (Fig. 2E). Decreased level of sgRNA accumulation subsequently affected the expression of CP as shown in the western blot depicted in Fig. 2F.

To further determine the importance of the first ACCA element located at nt 10–13 on PVX RNA accumulation in protoplasts we analyzed single and double nucleotide substitution mutants in the region including this element. Many single nt substitution mutations at positions 9–11 did not significantly affect plus-strand RNA accumulation, except for 9A to U, 10A to U, and 11C to A mutations. Although all single nt substitution mutations at nt positions 12 and 13 significantly

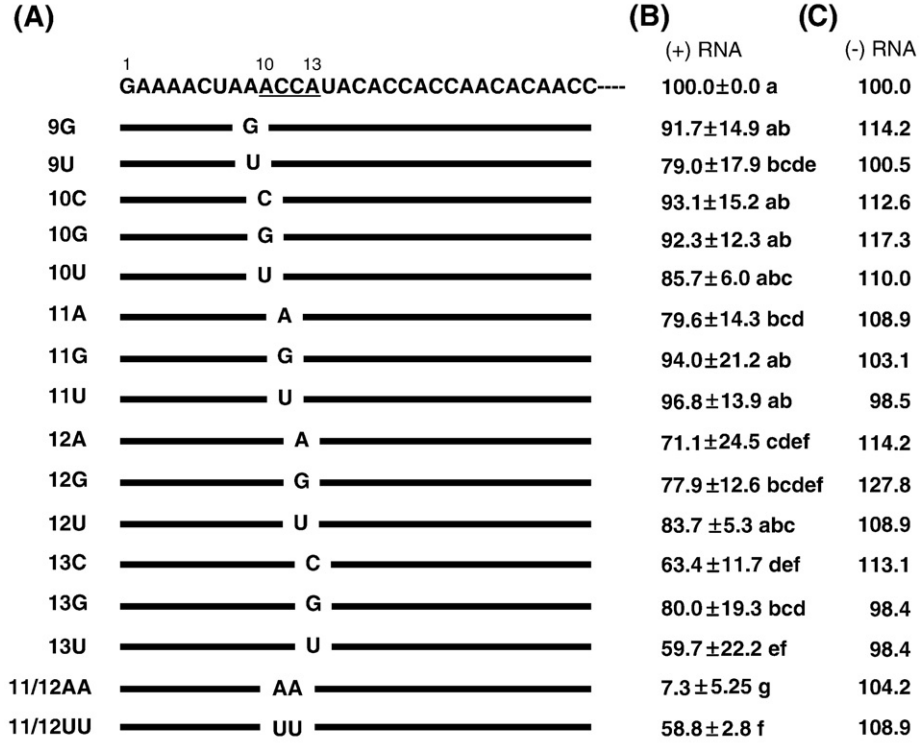

Fig. 3. Effects of single and double nucleotide mutations introduced into PVX genomic RNA on viral replication in *N. tabacum* NT1 protoplasts. (A) Schematic representation of mutations made in nt 9–13 containing the ACCA element of the PVX cDNA clone, pMON8453, using site-directed mutagenesis. (B) Accumulation of plus- and (C) minus-strand RNA on PVX mutants. RNA levels were measured using a Molecular Dynamics Photoimager. Each value is the mean compared to that of the wild type as a percentage of the wild type and the standard error compiled from at least six independent experiments for plus-strand RNA accumulation. Values with the same letter are not significantly different at $P \leq 0.05$. Since the accumulation of minus-strand RNA was not affected by the mutations introduced at the 5′ NTR (Kim and Hemenway, 1996, 1999; Miller et al., 1998; Fig. 1), minus-strand RNA accumulation levels were obtained from two independent experiments and are showing mean values.

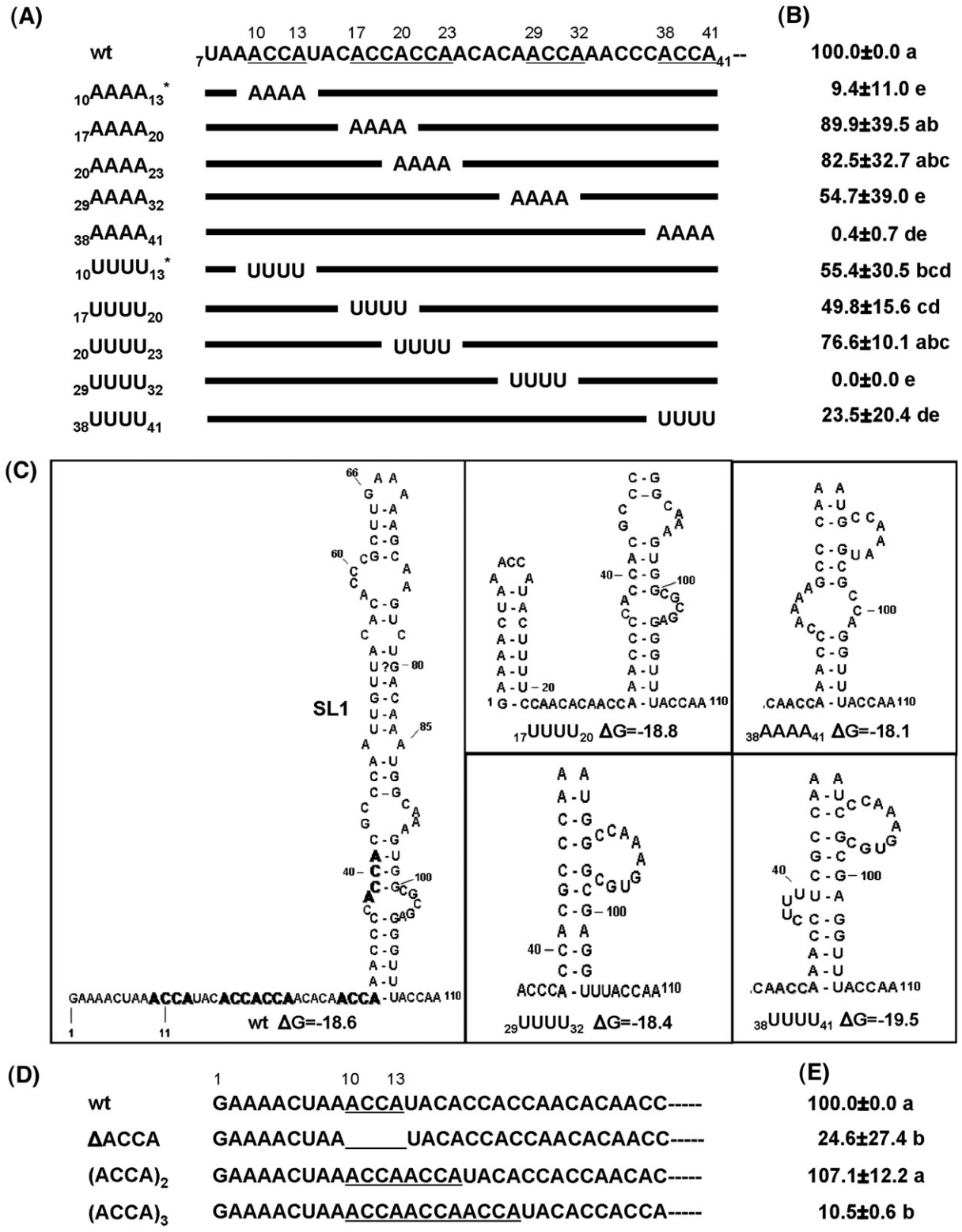

Fig. 4. Mutational analysis of five repeat ACCA sequences. (A and B) Schematic representation of mutations introduced in five repeat ACCA sequences at the 5′ end of PVX genomic RNA (A) and accumulation of progeny viral RNA (B). A total of 10 mutants changing each repeat ACCA sequence into AAAA or UUUU were inoculated into *N. benthamiana* plants. Two previously described mutants were also included in the analysis (asterisks; Kim et al., 2002). (C) Predicted secondary structure in the 5′ region of mutant viral RNA. The secondary structures of mutant RNA were predicted using the mFOLD program (http://www.bioinfo.rpi.edu/applications/mfold). The structural stability of each predicted RNA stem-loop structure is reflected in the given ΔG value. The predicted secondary structures for lower portion of SL1 in mutants $_{17}$UUUU$_{20}$, $_{29}$UUUU$_{32}$, $_{38}$AAAA$_{41}$, and $_{38}$UUUU$_{41}$ are shown since top portion of the predicted secondary structures of each mutant was identical. The predicted SL1 structures of mutants $_{10}$AAAA$_{13}$, $_{17}$AAAA$_{20}$, $_{20}$AAAA$_{23}$, $_{29}$AAAA$_{32}$, $_{10}$UUUU$_{13}$, and $_{29}$UUUU$_{32}$ were identical to that of wt. Repeated ACCA sequences are shown in bold character in the predicted secondary structure of wt. (D and E) Schematic representation of deletion and addition mutations introduced in the nt 10–13 ACCA sequence of the 5′ end of PVX genomic RNA (D) and accumulation of progeny viral RNA on upper systemic leaves (E). Total RNA was extracted from upper systemic leaves, and the relative accumulation of viral RNA was assayed using real-time-RT PCR as described in Materials and Methods. The average relative RNA accumulation and standard error were deduced from three independent experiments using three replicates of each sample. Values with the same letter are not significantly different at $P \leq 0.05$.

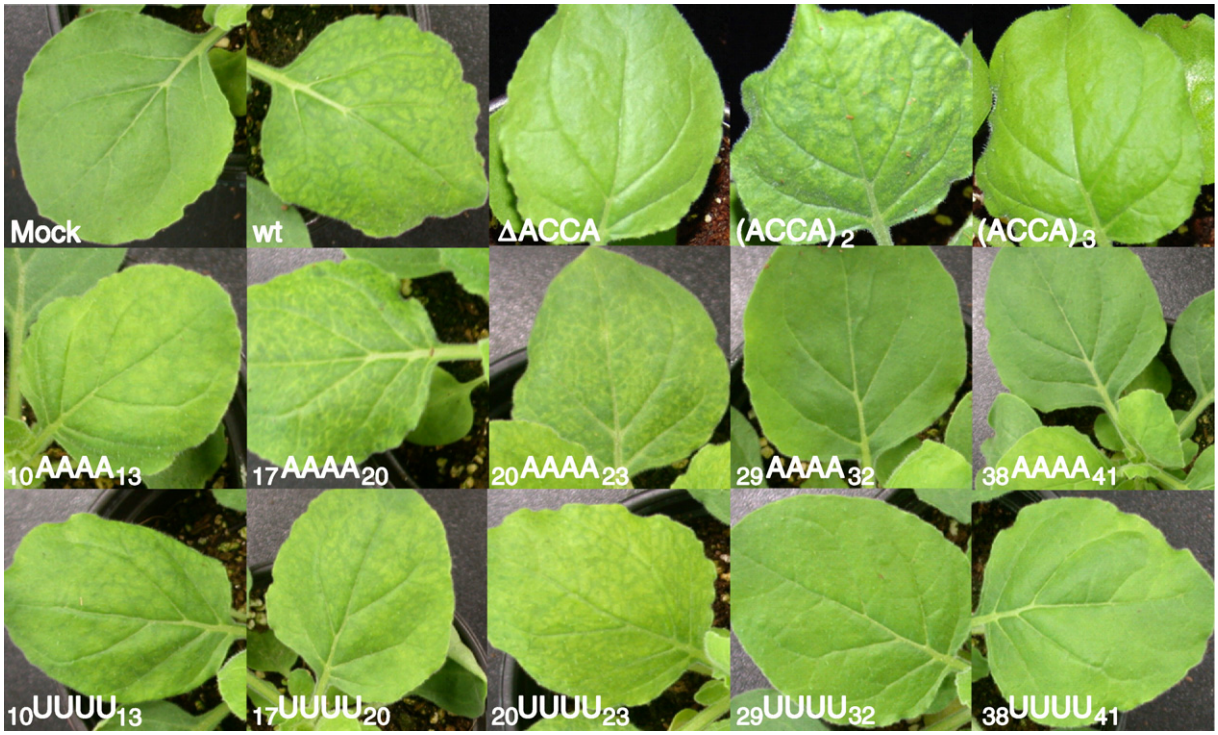

Fig. 5. Symptom development on upper systemic leaves of *Nicotiana benthamiana* plants inoculated with repeat ACCA mutated transcripts. Symptom development was observed for 14 days post-inoculation (dpi). The experiment was conducted more than three times using at least three plants for inoculation. Symptoms on each inoculated plant were summarized in Table 1.

decreased plus-strand RNA accumulation somewhat (Fig. 3), changing nt 11–12 CC into AA and UU had the greatest effect on plus-strand genomic RNA accumulation (Fig. 3B). Again, none of these mutations affected accumulation of genomic minus-strand RNA (Fig. 3C). Altogether, the deletion and site-directed mutation analyses indicated that the first ACCA element located at nt 10–13 of the PVX 5′ RNA is required for efficient plus-strand gRNA and sgRNA accumulation, but not for minus-strand RNA accumulation.

Effects of five repeated ACCA motifs located at the 5′ NTR of genomic RNA on PVX RNA replication

Given that the first ACCA element is important for plus-strand gRNA and sgRNA accumulation, we analyzed the other four ACCA elements located at nt 17–20, nt 20–23, nt 29–32, and nt 38–41 for their important to PVX replication (Fig. 4A). Therefore, to further determine whether the repeated ACCA motifs affect PVX RNA accumulation, we constructed 10 more site-directed mutants changing each ACCA sequence into AAAA and UUUU, determined their effects on PVX RNA accumulation by inoculating *N. benthamiana* plants with transcripts derived from the ACCA element mutants and wild-type PVX cDNA, and observed symptom development for 14 days post-inoculation (dpi). Severity of symptoms was qualitatively determined and designated by the number of plus signs, with symptoms in wild-type plants indicated by three plus signs. Plants inoculated with wt transcripts generally developed symptoms at 5–7 dpi (Fig. 5). When transcripts containing the $_{17}$UUUU$_{20}$ or $_{20}$UUUU$_{23}$ sequences were inoculated onto *N. benthamiana* plants, symptom development was similar to plants inoculated with wild-type transcripts. Vein banding and mosaic symptoms were observed on plants inoculated with the $_{17}$AAAA$_{20}$ or $_{20}$AAAA$_{23}$ mutant transcripts. In contrast, no symptoms were observed on plants inoculated with $_{38}$AAAA$_{41}$, $_{29}$UUUU$_{32}$ and $_{38}$UUUU$_{41}$ mutants at 7 dpi (Fig. 4 and Table 2). Replication of viruses, however, was observed on upper leaves, as confirmed by RT-PCR analysis (data not shown). Mild mosaic or mosaic symptoms were observed on plants inoculated with the $_{29}$AAAA$_{32}$, $_{10}$UUUU$_{13}$, and $_{17}$UUUU$_{20}$ mutant transcripts. Interestingly, we sometimes observed mild mosaic symptoms on plants inoculated with the $_{10}$AAAA$_{13}$ transcripts, which did not replicate efficiently on NT1 protoplasts; additional plant inoculations with these transcripts indicated symptom development on 5 out of 17 plants (29.4%; Table 2).

We have previously reported that the nucleotide changes in nt 10–13 ACCA into AAAA ($_{10}$AAAA$_{13}$) had a deleterious effect on PVX plus-strand RNA accumulation (5.3% compared to that of wt) and nt 10–13 ACCA into UUUU ($_{10}$UUUU$_{13}$) significantly reduced PVX plus-strand RNA accumulation (42.9% compared to that of wt), while there were no significant changes in genomic minus-strand RNA accumulation in inoculated NT1 protoplasts (Kim et al., 2002). To determine if the

Table 2
Symptom development on *Nicotiana benthamiana* plants inoculated with repeat ACCA mutated transcripts

Mutants	Symptoms	
Mock	0/9[a]	–[b]
Wild-type	9/9	SM, M
$_{10}$AAAA$_{13}$	5/17	MM, L
$_{17}$AAAA$_{20}$	6/9	VB, M, L
$_{20}$AAAA$_{23}$	9/9	VB, M
$_{29}$AAAA$_{32}$	3/16	MM, L
$_{38}$AAAA$_{41}$	0/9	L
$_{10}$UUUU$_{13}$	7/13	M, L
$_{17}$UUUU$_{20}$	5/13	M, L
$_{20}$UUUU$_{23}$	10/12	M, L
$_{29}$UUUU$_{32}$	0/12	L
$_{38}$UUUU$_{41}$	0/12	L
ΔACCA	3/9	MM, L
(ACCA)$_2$	8/9	SM,M, L
(ACCA)$_3$	4/9	M, L

[a] Symptom development was observed for 14 days post-inoculation (dpi). The experiment was conducted more than three times using at least three plants for inoculation. Numbers represent # of plants with visible symptom/# of inoculated plants.
[b] SM, severe mosaic; M, mosaic; MM, mild mosaic; VB, vein banding; L, latent infection; –, no infection.

severity of symptoms and the previous protoplast data would be reflected in PVX replication and in plant infection studies, respectively, accumulation of PVX RNAs on upper systemic leaves was obtained by real-time RT-PCR analyses. As shown in Fig. 4B, plants inoculated with mutants $_{10}$AAAA$_{13}$, $_{38}$AAAA$_{41}$, $_{29}$UUUU$_{32}$, and $_{38}$UUUU$_{41}$ exhibited dramatically decreased RNA accumulation (9.4%, 0.4%, 0.0%, and 23.5% compared to that of wt, respectively), while $_{29}$AAAA$_{32}$, $_{10}$UUUU$_{13}$, and $_{17}$UUUU$_{20}$ mutations resulted in moderate, but significant, reductions (54.7%, 55.4%, and 49.8% compared to that of wt, respectively). Plants inoculated with mutants $_{17}$AAAA$_{20}$, $_{20}$AAAA$_{23}$, and $_{20}$UUUU$_{23}$ accumulated reduced level, but not significantly different, of plus-strand RNA. The results showed close correlation between the level of plus-strand RNA replication in infected *N. benthamiana* plants and symptom development and reflection of the previously published protoplast data in plant infection studies at least for mutants $_{10}$AAAA$_{13}$ and $_{10}$UUUU$_{13}$ (Kim et al., 2002).

To determine whether mutated sequences were maintained in progeny viruses, we amplified the dsDNA-containing mutated region by RT-PCR and sequenced 10 independent clones from both inoculated and upper systemic leaf samples for each mutant. As in ACCA into AAAA mutations introduced at the first to fourth position, all mutated sequences maintained original mutations in all progeny clones tested (Tables 3 and 4). For the fifth ACCA to AAAA mutation, however, we found reversion of AAAA to ACCA in three of ten clones from upper systemic leaves, whereas progeny clones from inoculated leaves maintained the mutation. The sequence change at the fifth position (nt 38–41) was predicted to form a less stable secondary structure (Fig. 4C). Similarly, on analysis of the ACCA to UUUU mutant inoculated plants, recovered clones from progeny viruses had more sequence variations when introduced mutations caused changes in the predicted secondary structure of SL1 (Fig. 4C, Tables 3 and 4). These data suggest that RNA continues to evolve within inoculated plants to obtain an optimum template for PVX replication, in agreement with data of Miller et al. (1999) showing that sequence reversion and/or variation maintains suitable RNA secondary structure. These results indicate the importance of the first (10–13), fourth (29–32), and fifth (38–41) ACCA sequence motifs for viral replication.

Effects of deletions and insertions of ACCA at nt 10–13 on PVX replication

To determine the effect of deletions and insertions of ACCA at nt 10–13, we constructed three more mutants: one with mutant deletion of nt 10–13 (ΔACCA) and two adding either one or two ACCAs following the $_{10}$ACCA$_{13}$ ((ACCA)$_2$ and (ACCA)$_3$, respectively). Deletions and insertions of ACCA element at nt 10–13 did not affect the predicted SL1 structure. We determined the effect of these mutations on virus replication by inoculating the mutated transcripts onto *N. benthamiana* plants (Figs. 4D and 3E). Infection was monitored by evaluation of symptom development and detection of CP in inoculated and upper leaves. Plants inoculated with wt transcripts or with (ACCA)$_2$ mutant transcripts showed systemic symptoms by 5 to 7 dpi, and accumulated PVX CP in inoculated and upper leaves by 7 dpi in all 9 inoculated plants (Fig. 5 and data not shown). In contrast, plants inoculated with ΔACCA and (ACCA)$_3$ mutant transcripts did not develop symptoms in 6 and 5 out of 9 plants, respectively, for up to 14 dpi (Fig. 5) and did not contain detectable levels of CP at 7 dpi. The other plants, however, showed mild or no symptom development with virus replication. In general, mutants ΔACCA and (ACCA)$_3$ caused very weak symptom development with mild mosaic symptoms. Interestingly, the (ACCA)$_2$ mutant caused vein banding and mosaic symptom development while wt caused severe mosaic or mosaic symptoms at 7 dpi (Fig. 5 and Table 2). Total RNAs extracted from upper systemic leaves inoculated with transcripts of these mutations were analyzed for plus-strand RNA and CP accumulation. Plus-strand RNA accumulation in upper leaves inoculated with ΔACCA, (ACCA)$_2$ and (ACCA)$_3$ were 24.6%, 107.1% and 10.5% compared to that of wt (Fig. 4E). A correlation between plus-strand RNA accumulation and CP accumulation was observed (data not shown). Analysis of the sequences of the progeny viruses indicated that the mutated sequences were maintained in both inoculated and upper systemic leaves for ΔACCA and (ACCA)$_2$ mutants. In contrast, sequence conversion to the wt sequence was observed for the (ACCA)$_3$ mutant-inoculated plants. Altogether, these results indicate that the duplication of ACCA at nt 10–13, in mutant (ACCA)$_2$, did not significantly affect replication, whereas the deletion of ACCA or tripling of ACCA significantly reduced viral replication.

Table 3
Analysis of progeny viral RNA isolated from inoculated N. benthamiana leaves with repeat ACCA mutated transcripts

Mutants	Sequence[a]	# of clones[b]
$_{10}$AAAA$_{13}$	$_{8}$AAAAAUACACCACCAACACAACCAAACCCACCA——	(10/10)
$_{17}$AAAA$_{20}$	$_{8}$AACCAUACAAAACCAACACAACCAAACCCACCA——	(10/10)
$_{20}$AAAA$_{23}$	$_{8}$AACCAUACACCAAAAACACAACCAAACCCACCA——	(10/10)
$_{29}$AAAA$_{32}$	$_{8}$AACCAUACACCACCAACACAAAAAAACCCACCA——	(10/10)
$_{38}$AAAA$_{41}$	$_{8}$AACCAUACACCACCAACACAACCAAACCCAAAA——	(10/10)
$_{10}$UUUU$_{13}$	$_{8}$AUUUUUACACCACCAACACAACCAAACCCACCA——	(10/10)
$_{17}$UUUU$_{20}$	$_{8}$AACCAUACUCUUCCAACACAACCAAACCCACCA——	(6/10)
	$_{8}$AACCAUACUUUCCCAACACAACCAAACCCACCA——	(3/10)
	$_{8}$AACCAUACCUUUCCAACACAACCAAACCCACCA——	(1/10)
$_{20}$UUUU$_{23}$	$_{8}$AACCAUACACCUUUUACACAACCAAACCCACCA——	(10/10)
$_{29}$UUUU$_{32}$	$_{8}$AACCAUACACCACCAACACAUUUUAACCCACCA——	(9/10)
	$_{8}$AACCAUACACCACCAACACAACCACCCACCA——	(1/10)
$_{38}$UUUU$_{41}$	$_{8}$AACCAUACACCACCAACACAACCAAACCCUUUU——	(10/10)
ΔACCA	$_{8}$A____UACACCACCAACACAACCAAACCCACCA——	(10/10)
(ACCA)$_2$	$_{8}$AACCAACCAUACACCACCAACACAACCAAACCC——	(10/10)
(ACCA)$_3$	$_{8}$AACCAACCAACCAUACACCACCAACACAACCAA——	(8/10)
	$_{8}$AACCAUACACCACCAACACAACCAAACCCACCA——	(2/10)

[a] Sequences of recovered clones corresponding to the repeat ACCA sequence are underlined.
[b] The dsDNA-containing mutated region were amplified by RT-PCR and sequenced 10 independent clones for each mutant using total RNAs extracted at 7 dpi. Numbers represent # of clones for sequence analysis samples/ten clones.

Table 4
Analysis of progeny viral RNA isolated from upper systemic *N. benthamiana* leaves inoculated with repeat ACCA mutated transcripts

Mutants	Sequence[a]	# of clones[b]
Wild-type	$_{8}$AACCAUACACCACCAACACAACCAAACCCACCA——	
$_{10}$AAAA$_{13}$	$_{8}$AAAAAUACACCACCAACACAACCAAACCCACCA——	(10/10)
$_{17}$AAAA$_{20}$	$_{8}$AACCAUACAAAACCAACACAACCAAACCCACCA——	(10/10)
$_{20}$AAAA$_{23}$	$_{8}$AACCAUACACCAAAAACACAACCAAACCCACCA——	(10/10)
$_{29}$AAAA$_{32}$	$_{8}$AACCAUACACCACCAACACAAAAAAACCCACCA——	(10/10)
$_{38}$AAAA$_{41}$	$_{8}$AACCAUACACCACCAACACAACCAAACCCAAAA——	(7/10)
	$_{8}$AACCAUACACCACCAACACAACCAAACCCACCA——	(3/10)
$_{10}$UUUU$_{13}$	$_{8}$AUUUUUACACCACCAACACAACCAAACCCACCA——	(9/10)
	$_{8}$AUGUUUACACCACCAACACAACCAAACCCACCA——	(1/10)
$_{17}$UUUU$_{20}$	$_{8}$AACCAUACUUUUCCAACACAACCAAACCCACCA——	(3/10)
	$_{8}$AACCAUACUUUCCCAACACAACCAAACCCACCA——	(5/10)
	$_{8}$AACCAUACUCUUCCAACACAACCAAACCCACCA——	(1/10)
	$_{8}$AACCAUACAUAUCCAACACAACCAAACCCACCA——	(1/10)
$_{20}$UUUU$_{23}$	$_{8}$AACCAUACACCUUUUACACAACCAAACCCACCA——	(10/10)
$_{29}$UUUU$_{32}$	$_{8}$AACCAUACACCACCAACACAUUUUAACCCACCA——	(1/10)
	$_{8}$AACCAUACACCACCAACACAACCAAACCCACCA——	(9/10)
$_{38}$UUUU$_{41}$	$_{8}$AACCAUACACCACCAACACAACCAAACCCUUUU——	(8/10)
	$_{8}$AACCAUACACCACCAACACAACCAAACCCUCUU——	(2/10)
ΔACCA	$_{8}$A____UACACCACCAACACAACCAAACCCACCA——	(10/10)
(ACCA)$_2$	$_{8}$AACCAACCAUACACCACCAACACAACCAAACCC——	(10/10)
(ACCA)$_3$	$_{8}$AACCAACCAACCAUACACCACCAACACAACCAA——	(7/10)
	$_{8}$AACCAUACACCACCAACACAACCAAACCCACCA——	(3/10)

[a] Sequences of recovered clones corresponding to the repeat ACCA sequence are underlined.
[b] The dsDNA-containing mutated region were amplified by RT-PCR and sequenced 10 independent clones for each mutant using total RNAs extracted at 7 dpi. Numbers represent # of clones for sequence analysis samples/ten clones.

Discussion

Sequence comparisons of the ACCA motifs and the surrounding nucleotides indicate that the repeated ACCA sequences at the 5′ NTR are well conserved within PVX isolates, but less conserved within the

genus *Potexvirus* (Fig. 6; (Sit et al., 1994)). The ACCA sequence motif, however, is observed in many potexviruses, including *Clover yellow mosaic virus*, *Papaya mosaic virus*, *White clover mosaic virus*, *Narcissus mosaic virus*, and *Strawberry mild yellow edge virus*. The other potexviruses, including *Potato acuba mosaic virus*, *Plantago asiatica mosaic virus*, *Foxtail mosaic virus*, and *Bamboo mosaic virus*, do not contain the repeated ACCA motifs. Although all viruses do not contain the repeated ACCA motif(s), most viruses in the genus *Potexvirus* contain AC-rich sequences (Fig. 6B). Analyses of deletion and site-directed mutations introduced into the 5′ region of the PVX genome indicated that the first ACCA sequence element located at nt 10–13 of the 5′ RNA is required for efficient plus-strand genomic RNA and sgRNA accumulation, but not for minus-strand RNA synthesis. Mutations introduced into the second and the third ACCA motifs did not significantly affect virus replication or the development of symptoms in inoculated plants. Whereas most of the site-directed mutations introduced into nt position 9–13 affected PVX RNA replication to some extent, mutations that changed nt 11–12 CC into AA and UU severely affected plus-strand genomic RNA synthesis (Fig. 3). This is analogous to the significantly reduced or lack of accumulation of plus-strand RNA by the deletion of the first 11 or more nts (Fig. 2).

In this regard, it is worth nothing that the deletion of the first 8 nt (Δ8) or 9 nt (Δ9) from the 5′ end did not affect accumulation of PVX RNA levels; these mutants are predicted to maintain RNA–RNA interactions between terminal sequences, modeling 5′-terminal nt 4–11 and the 3′ hexanucleotide sequence element, and the internal conserved sequences located upstream of sgRNAs that are required for all PVX RNA accumulation (Hu et al., 2007; Kim and Hemenway, 1999), whereas a significantly reduced or no interaction was predicted with the deletion of 10 or more nts from the 5′ end of the PVX RNA (data not shown). When mutations affect RNA–RNA long-distance interactions, e.g., 11–12 AA and UU, such that the normal RNA–RNA base-pairing between the 5′ terminus (or 3′ terminus of minus-strand RNA) and the conserved octanucleotide elements is reduced compared to that of the wt, sgRNA and gRNA syntheses are reduced. These results indicate the importance of multiple RNA–RNA long-distance interactions (Fig. 1B) and correlate with results previously observed for plus-strand RNA accumulation *in vivo*. RNA–RNA interactions and the dynamic RNA conformations as important regulators of virus replication were also reported in several other systems (Alvarez et al., 2005; Olsthoorn et al., 1999; Ray et al., 2003; Zhang et al., 2006). It is possible that these RNA interactions may also regulate other important virus life cycle phases, including translation, assembly, and switches in these important steps.

To further clarify the importance of the first ACCA motif, we tested the effect of deletion (ΔACCA) and insertions ($(ACCA)_2$ and $(ACCA)_3$) of ACCA. Although the deletion of one and the insertion of two ACCA sequence elements significantly affected RNA accumulation and symptom development, the insertion of one ACCA ($(ACCA)_2$) led to the accumulation of comparable RNA and caused vein banding and mosaic symptom compared to those of the wt (Fig. 5 and Table 2). A cellular protein, p54, binds to the 5′ NTR of plus-strand RNA and determines the nt 10–13 ACCA at the 5′ NTR of PVX RNA, affecting the binding of a 54-kDa protein *in vitro* and RNA accumulation in protoplasts (Kim et al., 2002). The effects of host protein binding to these ACCA deletion and insertion mutants, however, have not yet been defined and will shed light on the importance of the ACCA motif in host protein binding. These results support the proposal that the nt 10–13 ACCA element at the 5′ NTR of the PVX region may be involved in RNA–RNA and RNA–protein interactions that are required for PVX replication.

A stem-loop structure (SL1), which forms within nt 32–106 in the 5′ region of PVX RNA, is critical for the life cycle of PVX in host plants. Various features of a stable SL1 are important for replication (Miller et al., 1998, 1999) and the formation of virus-like particles by providing the

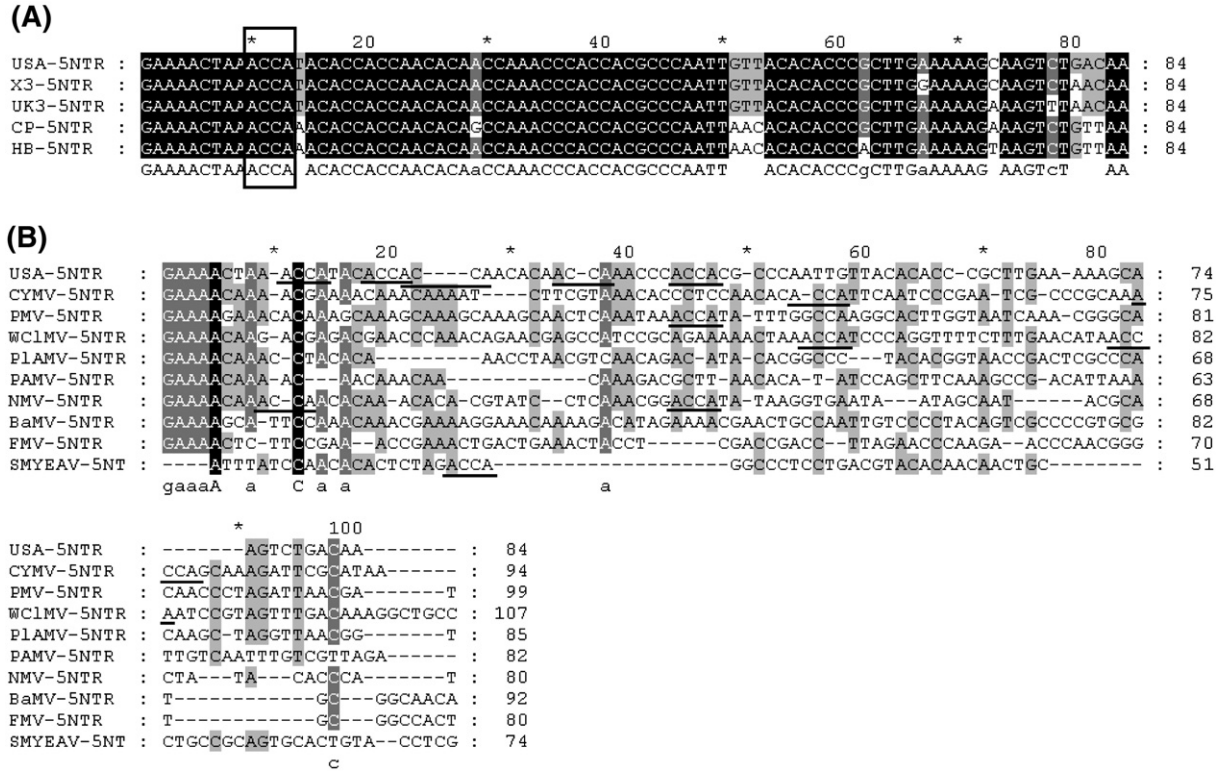

Fig. 6. Multiple sequence alignments of nucleotide sequences at the 5′ NTR of PVX isolates (A) and of the genus *Potexvirus* (B). Numbers at the top represent the nucleotide position of each isolate. Nucleotide sequences: PVX-USA (Hemenway et al., 1990), PVX-X3 (D00344), PVX-UK3 (AY297843), PVX-CP (X55802), PVX-HB (X72214), *Clover yellow mosaic virus* (D29630), *Papaya mosaic virus* (D13957), *White clover mosaic virus* (X16636), *Plantago asiatica mosaic virus* (Z21647), *Potato acuba mosaic virus* (S73580), *Narcissus mosaic virus* (D13747), *Bamboo mosaic virus* (L77962), *Foxtail mosaic virus* (M62730), and *Strawberry mild yellow edge virus* (D12517).

specific recognition site for the CP subunit (Kwon et al., 2005). The SL1 is also implicated as the signal for cell-to-cell movement of PVX RNA (Lough et al., 2006). Although we have not looked for second site reversions that may also affect the fitness of progeny RNA, our data indicate that the preferred RNA sequence and structural elements of SL1 are selected for during PVX replication, as suggested previously (Miller et al., 1999). It is also possible that SL1 might provide a specific binding site for host factors that might play a role in modulating the virus replication cycle by interacting with viral protein(s) and other host factors. In this regard, it is worth mentioning that several host factors specifically recognize and interact with SL1 formed in both plus- and minus-strand RNA (S.-Y. Cho and K.-H. Kim, unpublished data). The characterization of these host factors and determination of their possible roles in modulating the virus replication cycle remain to be performed.

We characterized the functional significance of the repeated ACCA sequence elements at the 5′ NTR region in PVX replication by introducing substitution, deletion, and addition mutations into the repeated ACCA element in the 5′ NTR of the PVX RNA. We showed the importance of the first ACCA element for PVX replication. Because the binding of the cellular protein to the 5′ region of PVX RNA and virus replication in inoculated protoplasts were closely correlated to p54 binding to the 5′ end of plus-strand RNA, it is tempting to speculate that the requirement for sequences on the 5′ end of PVX RNA is in part due to the binding of cellular protein, as well as CP subunits. It is also possible that different cellular proteins recognize and bind PVX regulatory elements located at the PVX 5′ and 3′ ends and elsewhere on PVX RNA to allow virus replication and to modulate the virus life cycle. Future experiments will involve the characterization of each cellular protein interaction with PVX RNA and/or with viral and other cellular proteins.

Materials and methods

Plasmid construction and in vitro transcription

Mutations were introduced into the PVX cDNA clone pMON8453 (Hemenway et al., 1990) using the muta-Gene *in vitro* mutagenesis kit (Bio-Rad) (Kunkel, 1985). Construction of the control plasmid p32 was described previously (Kim and Hemenway, 1996). All site-directed mutants were verified by sequencing, and a region containing the mutation was resected back into a wt pMON8453 clone. The resulting clones were sequenced through the entire resected fragment and flanking regions to ensure that only the introduced mutations were present. *In vitro* transcription reactions were performed as described previously (Kim and Hemenway, 1996). The quality and relative concentration of transcripts was checked by electrophoresis on 1% agarose gel at 4 °C, and visualized by ethidium bromide staining.

S1 nuclease protection assay

Total RNA was isolated from inoculated protoplasts using Trizol reagent (Molecular Research Center, Inc., USA) at 48 hpi. S1 nuclease protection assays were used to detect minus- and plus-strand PVX RNA, with single-stranded DNA probes (Kim and Hemenway, 1996, 1997). The products from S1 nuclease digestion were separated on 6% sequencing gel and visualized by autoradiography. The relative molar amounts of PVX RNA in each sample were determined using Image Quant software on a Molecular Dynamics Phosphoimager.

Northern blotting

Total RNA was isolated from inoculated protoplasts using Trizol reagent (Molecular Research Center, Inc., USA) at 48 hpi. Total RNA was electrophoresed on 1% denaturing gel and blotted onto nylon transfer membranes (Amersham Biosciences). The blots were probed with ^{32}P-labeled PVX CP fragments.

Western blotting

At 48 hpi, 10^5 protoplasts from 7 dpi plants were resuspended in 30 μl of Laemmli loading buffer (Laemmli, 1970), electrophoresed on 12% SDS-polyacrylamide gel, and blotted onto PVDF transfer membranes (Amersham Biosciences, USA; (Towbin et al., 1992).The blots were probed with antiserum prepared against purified PVX. The products were visualized using a Biotin/StreptAvidin kit (Amersham Biosciences, USA).

Protoplast and plant inoculations

Capped transcripts (5 μg) derived from pMON8453 or mutant clones were resuspended in 0.1 M phosphate buffer (pH 8.0) and inoculated onto two leaves of *N. benthamiana* plants (Hemenway et al., 1990). Inoculated plants were maintained under a photocycle of 25 °C for 12 h in the light and at 22 °C for 12 h in the dark and were monitored for symptom development for up to 2 weeks post-inoculation. For protoplast inoculation, capped transcripts (5 μg) derived from pMON8453 or mutant clones were resuspended in DEPC-dH_2O and inoculated into NT1 protoplast as described previously (Kim and Hemenway, 1997).

RT-PCR and sequencing

Total RNA was isolated from mock and ACCA mutant transcript-inoculated *N. benthamiana* plants using Trizol reagent (Molecular Research Center, Inc., USA) according to the manufacturer's protocol. RT-PCR was performed as described previously (Ko et al., 2007) using PVX 5′pr1 (5′-GAAAACTAA-3′), PVX 5′pr2 (5′-GAAAACTAAACCATA-CAC-3′), and PVX 3′pr (5′-CTATAAGCCTCATCTTG-3′), which are complementary to nucleotides 1–9, 1–18, and 161–145, respectively. The PCR conditions were: one cycle at 94 °C for 5 min; 30 cycles of 94 °C for 30 s, 50 °C for 1 min, and 72 °C for 1 min; and one cycle of elongation at 72 °C for 10 min. The amplified DNA fragments were cloned into the pGEM-T EASY vector (Promega, USA). Inserts were sequenced using the dideoxynucleotide chain termination method, using the ABI Prism 3730 XL DNA Analyzer (PE Applied Biosystems, USA) located at the NICEM (Seoul National University).

Real-time RT-PCR

Real-time RT-PCR was performed on the Applied Biosystems 7500 Fast Real-Time PCR System (Applied Biosystems, USA) using cDNA synthesized from Turbo DNA-*free*™ (Ambion, Inc., USA) -treated total RNA using the fluorescent SYBR green method. The real-time PCR reaction was done in a total volume of 10 μl containing 5 μl of SYBR® Green PCR Master Mix (Applied Biosystems, USA), 20 ng of cDNA, and a final concentration of 200 nM primers (PVX-F; 5′-GCCCAATTGTTA-CACACC-3′ and PVX-R; 5′-CTATAAGCCTCATCTTG-3′), which are complementary to nucleotides 44–60 and 161–145, respectively. The PCR reactions were: 50 °C for 2 min and 95 °C for 10 min; 40 cycles of 95 °C for 15 s and 60 °C for 1 min; and finally, 72 °C for 10 min. Immediately after the final PCR cycle, melting curve analysis was conducted to determine the specificity of the reaction by incubating the reaction at 95 °C for 15 s, annealing at 60 °C for 20 s, and then slowly increasing the temperature to 95 °C over 20 min. PVX RNA accumulation was normalized to the ubiquitin 3 (Ubi3) endogenous gene (Rotenberg et al., 2006). Threshold values for threshold cycle (C_t) determination were generated automatically by the Applied Biosystem Detection v 1.3.1 software. Lack of variation in PCR products and the absence of primer–dimers were ascertained from the melt curve profile of the PCR products.

Computer-aided analysis of progeny RNA

RNA secondary structures were predicted using the mFOLD program (http://www.bioinfo.rpi.edu/applications/mfold; (Mathews et al., 1999;

Zuker, 1989) using sequences of progeny viral RNA obtained from inoculated and upper systemic leaves.

Statistical analysis

Data were statistically analyzed by analysis of variance (ANOVA) and means were compared using the Fisher's LSD (Least significant difference) test. Statistical analysis was performed with SAS (version 9.1; SAS Institute Inc., USA).

Acknowledgments

This research was supported in part by grants from a National Institutes of Health Grant GM49841 awarded to CH; the Center for Plant Molecular Genetics and Breeding Research funded by the MEST of the Republic of Korea; the Agriculture Specific Research Project funded by the Rural Development Administration; the Korea Science and Engineering Foundation (KOSEF) grant funded by the Korea government (MEST) (No. R01-2008-000-10087-0) to KHK; and by a Korea Research Foundation Grant funded by the Korean Government (MOEHRD, Basic Research Promotion Fund) (KRF-2005-217-F00001) to SJK. MRP was supported by graduate fellowship from the Ministry of Education through the Brain Korea 21 Project.

References

Alvarez, D.E., Lodeiro, M.F., Luduena, S.J., Pietrasanta, L.I., Gamarnik, A.V., 2005. Long-range RNA–RNA interactions circularize the dengue virus genome. J. Virol. 79, 6631–6643.

Argos, P., Tsukihara, T., Rossmann, M.G., 1980. A structural comparison of concanavalin A and tomato bushy stunt virus protein. J. Mol. Evol. 15, 169–179.

Bercks, R., 1970. Potato virus X. CMI/AAB descriptions of plant viruses. Commomwealth, Kew. England no. 111.

Chapman, S., Kavanagh, T., Baulcombe, D., 1992. Potato virus X as a vector for gene expression in plants. Plant J. 2, 549–557.

Dolja, V.V., Grama, D.P., Morozov, S.Y., Atabekov, J.G., 1987. Potato virus X-related single- and double-stranded RNAs. FEBS Lett. 214, 308–312.

Hemenway, C., Weiss, J., O'Connell, K., Tumer, N.E., 1990. Characterization of infectious transcripts from a potato virus X cDNA clone. Virology 175, 365–371.

Hu, B., Pillai-Nair, N., Hemenway, C., 2007. Long-distance RNA–RNA interactions between terminal elements and the same subset of internal elements on the potato virus X genome mediate minus- and plus-strand RNA synthesis. RNA 13, 267–280.

Huisman, M.J., Linthorst, H.J., Bol, J.F., Cornelissen, J.C., 1988. The complete nucleotide sequence of potato virus X and its homologies at the amino acid level with various plus-stranded RNA viruses. J. Gen. Virol. 69, 1789–1798.

Karpova, O.V., Arkhipenko, M.V., Zaiakina, O.V., Nikitin, N.A., Kiseleva, O.I., Kozlovskii, S.V., Rodionova, N.P., Atabekov, I.G., 2006. [Translational regulation of potato virus X RNA-coat protein complexes: the key role of a coat protein N-terminal peptide]. Mol. Biol. (Mosk) 40, 703–710.

Kim, K.-H., Hemenway, C.L., 1996. The 5′ nontranslated region of potato virus X RNA affects both genomic and subgenomic RNA synthesis. J. Virol. 70, 5533–5540.

Kim, K.-H., Hemenway, C.L., 1997. Mutations that alter a conserved element upstream of the potato virus X triple block and coat protein genes affect subgenomic RNA accumulation. Virology 232, 187–197.

Kim, K.-H., Hemenway, C.L., 1999. Long-distance RNA–RNA interactions and conserved sequence elements affect potato virus X plus-strand RNA accumulation. RNA 5, 636–645.

Kim, K.-H., Kwon, S.-J., Hemenway, C.L., 2002. Cellular protein binds to sequences near the 5′ terminus of potato virus X RNA that are important for virus replication. Virology 301, 305–312.

Ko, S.-J., Lee, Y.-H., Cho, M.-S., Park, J.-W., Choi, H.-S., Lim, G.-C., Kim, K.-H., 2007. The incidence of virus diseases on melon in Jeonnam province during 2000–2002. Plant Pathol. J. 23, 215–218.

Kunkel, T.A., 1985. Rapid and efficient site-specific mutagenesis without phenotypic selection. Proc. Natl. Acad. Sci. U. S. A. 82, 488–492.

Kwon, S.-J., Park, M.-R., Kim, K.-W., Plante, C.A., Hemenway, C.L., Kim, K.-H., 2005. *cis*-Acting sequences required for coat protein binding and in vitro assembly of Potato virus X. Virology 334, 83–97.

Laemmli, U.K., 1970. Cleavage of structural proteins during the assembly of the head of bacteriophage T4. Nature 227, 680–685.

Lough, T.J., Lee, R.H., Emerson, S.J., Forster, R.L., Lucas, W.J., 2006. Functional analysis of the 5′ untranslated region of potexvirus RNA reveals a role in viral replication and cell-to-cell movement. Virology 351, 455–465.

Mathews, D.H., Sabina, J., Zuker, M., Turner, D.H., 1999. Expanded sequence dependence of thermodynamic parameters improves prediction of RNA secondary structure. J. Mol. Biol. 288, 911–940.

Miller, E.D., Kim, K.-H., Hemenway, C.L., 1999. Restoration of a stem-loop structure required for potato virus X RNA accumulation indicates selection for a mismatch and a GNRA tetraloop. Virology 260, 342–353.

Miller, E.D., Plante, C.A., Kim, K.H., Brown, J.W., Hemenway, C.L., 1998. Stem-loop structure in the 5′ region of Potato virus X genome required for plus-strand RNA accumulation. J. Mol. Biol. 284, 591–608.

Morozov, S., Miroshnichenko, N.A., Solovyev, A.G., Fedorkin, O.N., Zelenina, D.A., Lukasheva, L.I., Karasev, A.V., Dolja, V.V., Atabekov, J.G., 1991. Expression strategy of the potato virus X triple gene block. J. Gen. Virol. 72, 2039–2042.

Olsthoorn, R.C., Mertens, S., Brederode, F.T., Bol, J.F., 1999. A conformational switch at the 3′ end of a plant virus RNA regulates viral replication. EMBO J. 18, 4856–4864.

Oparka, K.J., Roberts, A.G., Roberts, I.M., Prior, D.A.M., Crus, S.S., 1996. Viral coat protein is targeted to, but does not gate, plasmodesmata during cell-to-cell movement of potato virus X. Plant J. 10, 805–813.

Price, M., 1992. Examination of potato virus X proteins synthesized in infected tobacco plants. J. Virol. 66, 5658–5661.

Ray, D., Wu, B., White, K.A., 2003. A second functional RNA domain in the 5′ UTR of the Tomato bushy stunt virus genome: intra- and interdomain interactions mediate viral RNA replication. RNA 9, 1232–1245.

Rotenberg, D., Thompson, T.S., German, T.L., Willis, D.K., 2006. Methods for effective real-time RT-PCR analysis of virus-induced gene silencing. J. Virol. Methods 138, 49–59.

Rozanov, M.N., Koonin, E.V., Gorbalenya, A.E., 1992. Conservation of the putative methyltransferase domain: a hallmark of the 'Sindbis-like' supergroup of positive-strand RNA viruses. J. Gen. Virol. 73, 2129–2134.

Sit, T.L., Leclerc, D., AbouHaidar, M.G., 1994. The minimal 5′ sequence for in vitro initiation of papaya mosaic potexvirus assembly. Virology 199, 238–242.

Skryabin, K.G., Morozov, S., Kraev, A.S., Rozanov, M.N., Chernov, B.K., Lukasheva, L.I., Atabekov, J.G., 1988. Conserved and variable elements in RNA genomes of potexviruses. FEBS Lett. 240, 33–40.

Towbin, H., Staehelin, T., Gordon, J., 1992. Electrophoretic transfer of proteins from polyacrylamide gels to nitrocellulose sheets: procedure and some applications. Biotechnology 24, 145–149.

Verchot, J., Angell, S.M., Baulcombe, D.C., 1998. In vivo translation of the triple gene block of potato virus X requires two subgenomic mRNAs. J. Virol. 72, 8316–8320.

Zhang, J., Zhang, G., Guo, R., Shapiro, B.A., Simon, A.E., 2006. A pseudoknot in a preactive form of a viral RNA is part of a structural switch activating minus-strand synthesis. J. Virol. 80, 9181–9191.

Zuker, M., 1989. Computer prediction of RNA structure. Methods Enzymol. 180, 262–288.